Section 4: **Focus on select example applications of nanoscience in energy, environment, and health**

Yeshu Tan, Ivan P. Parkin, Guanjie He

Chapter 4A
Electrocatalytic hydrogen production

Abstract: Hydrogen is a clean energy alternative to adjust and interconnect the energy landscape as it is renewable, cost-effective, and relatively easily processed. The rapid development of advanced materials and deep mechanistic studies for electrocatalytic processes provides a good backdrop for developing more efficient hydrogen generation. This chapter summarizes the development of hydrogen energy, current research progress in electrocatalytic hydrogen evolution, and advanced materials in hydrogen production, storage, and utilization.

Keywords: hydrogen development, hydrogen evolution reaction, electrocatalyst, electrocatalytic water splitting, hydrogen storage

4A.1 Hydrogen energy and development

Fossil fuel consumption has led to emissions of polluting gases that have led to a global warming crisis. This has been driven by rapid economic development that has led to a doubling of global energy requirements over the last 30 years [1]. Greenhouse gases are mainly generated from carbon-containing sources and have accelerated climate change. Moreover, other pollution gases containing sulfur and nitrogen are hazardous to humans and the environment [2]. Thus, more and more countries have announced guidelines for developing clean energy systems, including solar energy, wind energy, tidal power, and geothermal energy [3]. These renewable energy sources rely on natural phenomena, such as solar and wind, which are intermittent. Nuclear power is also a suitable alternative to fossil fuels but risks widespread

Acknowledgments: The authors acknowledge the Engineering and Physical Sciences Research Council (EPSRC, EP/V027433/1, EP/L015862/1) and the Royal Society (RGS\R1\211080; IEC\NSFC\201261) for the funding support.

Yeshu Tan, Christopher Ingold Laboratory, Department of Chemistry, University College London, 20 Gordon Street, London WC1H 0AJ, United Kingdom, e-mail: yeshu.tan.19@ucl.ac.uk
Guanjie He, Christopher Ingold Laboratory, Department of Chemistry, University College London, 20 Gordon Street, London WC1H 0AJ, United Kingdom, e-mail: yeshu.tan.19@ucl.ac.uk; School of Chemistry, University of Lincoln, Joseph Banks Laboratories, Green Lane, Lincoln, LN6 7DL, United Kingdom, e-mail: g.he@ucl.ac.uk
Ivan P. Parkin, Christopher Ingold Laboratory, Department of Chemistry, University College London, 20 Gordon Street, London WC1H 0AJ, United Kingdom, e-mail: i.p.parkin@ucl.ac.uk

https://doi.org/10.1515/9783110739879-010

damaging leaks (Chernobyl, Fujishima). Further, nuclear waste disposal is a significant problem. It is perhaps not a safe alternative for long-term energy needs, but it has the short-term advantage of not producing climate-damaging gases [4].

Due to the different usage of electricity between days and nights, batteries, pump storage, or other energy vectors such as hydrogen could hold the key to widespread renewable energy usage. As clean energy, hydrogen is widely regarded as a promising, cost-effective, environment-friendly energy alternative to fossil fuels [5, 6]. Hydrogen can be produced from water, plants, and geothermal processes, which are fairly evenly distributed worldwide, unlike the distribution of fossil fuel sources. Developing clean energy can mitigate the energy shortage for those areas relying heavily on imported fossil fuels. Hydrogen has a high energy density (142 MJ/kg), and proton-exchange hydrogen fuel cells are promising devices for utilizing hydrogen, and the only by-product is water [7, 8]. Hydrogen can also be stored in tanks and transferred through pipes like natural gas to the energy area [9]. The increasing trends of interest in hydrogen energy are becoming more practical for the programs carried out in many countries [10]. The related utilization of hydrogen energy has been achieved, such as in fuel-cell cars [11]. The hydrogen system consists of production, storage, and application and will become more and more important for future energy systems [12].

Continuous and stable hydrogen production is required for the hydrogen economy. The main methods to produce hydrogen are steam reforming and electrochemical water splitting. The steam-methane reforming method is now the cheapest and the most mature way to produce hydrogen. However, the reactions occur at high temperatures and form by-product CO, making the process environmentally damaging [13]. A different reaction is needed to transfer CO to CO_2, increasing energy consumption and releasing greenhouse gases. The reaction of steam-methane reforming is carried out at around 700 °C, assisted by a catalyst:

$$CH_4 + H_2O = CO + 3H_2 \tag{4A.1}$$

Carbon monoxide is a toxic by-product, which is often converted to carbon dioxide with further oxidation by an excess of steam:

$$CO + H_2O = CO_2 + H_2 \tag{4A.2}$$

The whole reaction of steam-methane reforming is described as follows:

$$CH_4 + 2H_2O = CO_2 + 4H_2 \tag{4A.3}$$

The problems with the steam-methane process include catalyst poisoning by CO and the necessary purification of hydrogen from the gas mixture [14]. The poisoning is inevitable and leads to a decrease in production efficiency. The purification process is based on membranes with selective transport, which increases the cost. The whole process makes steam-methane reforming much more complicated than electrochemical water splitting. Besides the production efficiency, the safety issues are significant during steam-methane reforming.

The purity of hydrogen produced from electrochemical water splitting is comparatively high, with oxygen being formed at the other electrode, reflected by the equation:

$$2H_2O = 2H_2 + O_2 \quad (4A.4)$$

The schematic illustration of electrochemical water splitting is shown in Fig. 4A.1.

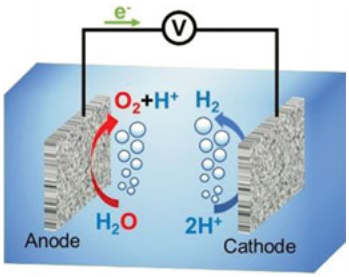

Fig. 4A.1: Schematic illustration of electrochemical water splitting.

The hydrogen can be directly collected from electrochemical water splitting. With the assistance of a membrane during the reaction, the purification process is quite simple. However, electrical consumption for water splitting is significantly higher than the estimated energy utilization of the produced hydrogen, which means that the hydrogen usage directly from water splitting is not that economical [15]. Electrochemical water splitting is an alternative to transfer excess power to hydrogens, such as electrical power from solar energy, tidal energy, and wind energy. These natural energy sources are unstable and intermittent, which is not optimal for long-term continuous output. Thus, water splitting can be an easy and excellent method to store the energy as hydrogen, which is environmental-friendly and mobile. To reduce the cost of electrochemical water splitting, photocatalytic water splitting is becoming popular, acquiring energy from the Sun. However, the transfer efficiency is relatively low, combined with electrocatalytic water splitting [16].

4A.2 Electrocatalytic hydrogen evolution reaction

Electrocatalysis is the foundation of hydrogen-based renewable and green energy conversion systems. Many devices and applications rely on hydrogen as an energy vector, including the petroleum refining industry, fuel cells, and the synthesis of ammonia [17, 18]. Therefore, the electrocatalytic hydrogen evolution reaction (HER) has increased attention over recent years.

Nowadays, electrocatalytic HER in the alkaline electrolyte is widely studied and applied commercially. It has relatively low cost and excellent gas generation efficiency [19]. The hydrogen can be easily collected with high purity using a simple proton-conduction membrane. The reaction mechanism of hydrogen evolution on

the cathode includes three steps such as the Volmer step, the Heyrovsky step, and the Tafel step, involving hydrogen intermediates (*H) adsorption and desorption. When the reaction is performed in a neutral and basic environment, the first step is dissociating water molecules in the Volmer step, as described below. Then hydrogen is produced through either the Heyrovsky step or the Tafel step:

$$\text{catalyst} + H_2O + e^- = \text{catalyst} - {}^*H + OH^- \ (\text{Volmer step})$$

$$\text{catalyst} - {}^*H + H_2O + e^- = \text{catalyst} + H_2 + OH^- \ (\text{Heyrovsky step})$$

$$2\,\text{catalyst} - {}^*H \rightarrow 2\,\text{catalyst} + H_2 \ (\text{Tafel step})$$

When the hydrogen evolution happens in acidic media, the reaction pathway is similar, except the dissociation of water occurs in the Volmer step. The hydrogen intermediates are formed in the Volmer step, and then the pathway undergoes a Heyrovsky step, or Tafel step, to form hydrogen:

$$H^+ + e^- + \text{catalyst} = \text{catalyst} - {}^*H \ (\text{Volmer step})$$

$$\text{catalyst} - {}^*H + e^- + H^+ = \text{catalyst} + H_2 \ (\text{Heyrovsky step})$$

$$2\,\text{catalyst} - {}^*H \rightarrow 2\,\text{catalyst} + H_2 \ (\text{Tafel step})$$

The reaction steps are different because of the H^+ or OH^- domination in acidic or basic electrolytes, which also influences hydrogen production efficiency, as shown in the schematic illustration of HER steps in Fig. 4A.2. The adsorption and desorption of *H on the catalyst are significant for hydrogen evolution, which can be the rate-determining steps.

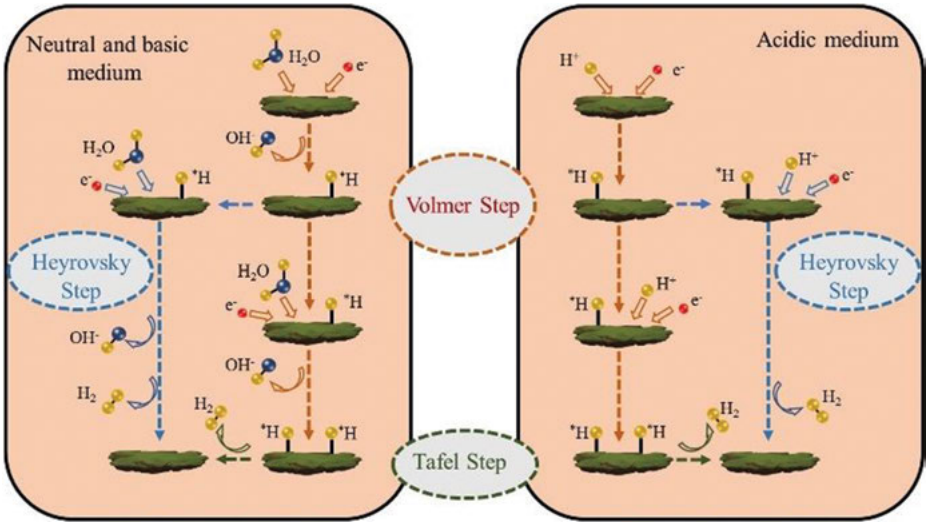

Fig. 4A.2: Schematic illustration of three steps of hydrogen evolution reaction in different media.

Suitable hydrogen bond formation can encourage an efficient HER process. H-bonding can limit the pathway to either weak or strong, making the useful description of hydrogen adsorption energy (ΔG_H) close to zero. The schemes shown in Fig. 4A.3 provide guidelines for the metal material design according to the changes in ΔG_H [20]. The volcano plot shows the inherent advantages of noble metal for the appropriate ability to promote HER catalysis.

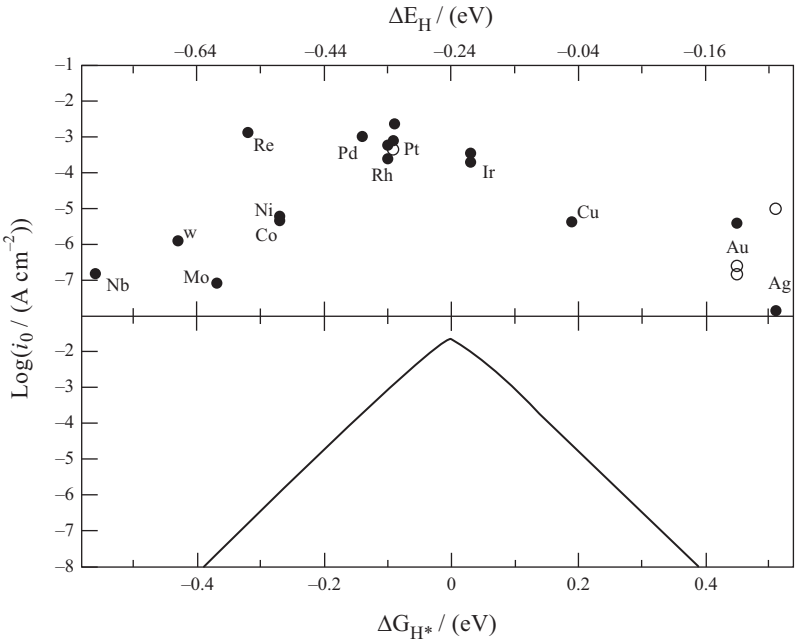

Fig. 4A.3: (Top) Experimentally measured exchange current, log(i_0), for hydrogen evolution over different metal surfaces plotted as a function of the calculated hydrogen chemisorption energy per atom, $\triangle E_H$ (top axis); (bottom) the result of the simple kinetic model is plotted as a function of the free energy for hydrogen adsorption [20] (Copyright 2005, Institute of Physics).

The increasing research interest in HER has accelerated the development of electrocatalysts. Electrocatalysts with lower overpotential and enhanced stability are desirable to promote applications and devices relying on hydrogen. This has promoted various synthesis methods.

4A.3 Advanced materials in hydrogen production

HER from water electrolysis is a promising strategy for producing clean hydrogen. Many challenges need to be overcome to lower the overpotential and accelerate the

HER kinetics in different media. Thus, for realizing efficient HER, numerous kinds of catalysts have been developed, including noble-metal, transition-metal-based, and metal-free electrocatalysts, which show promising performances and specific advantages for HER [21, 22].

4A.3.1 Noble-metal-based electrocatalyst

Noble metals, especially Pt, have attracted attention due to their intrinsic efficient HER properties. The inherent hydrogen adsorption energy which is close to zero makes it a promising candidate as an HER catalyst. However, the limitation and expense of precious metal sources restrict their use as electrocatalysts. Therefore, researchers have developed various kinds of methods to modify the materials. Figure 4A.4 illustrates the schematic of three main ways of structural regulation of noble-metal electrocatalysts, including shape modification, alloy composition, and single atom incorporation.

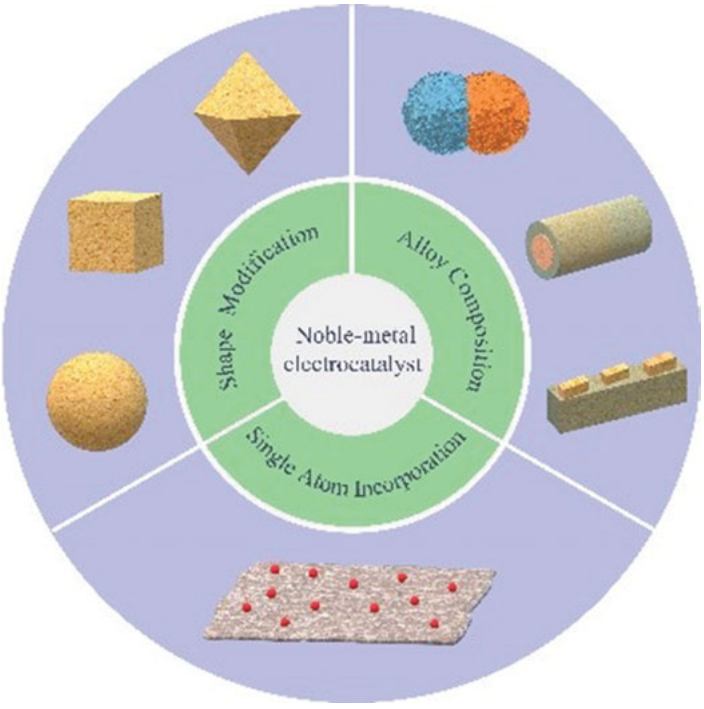

Fig. 4A.4: Schematic illustration of three ways of utilization of noble-metal electrocatalysts.

One possible way is to adjust the shape of the noble-metal nanoparticles to achieve a large specific surface area and high density of electrocatalytic sites. Among noble-metal electrocatalysts, platinum-based electrocatalysts are considered the best performance for HER. Different strategies have been developed to synthesize numerous catalyst shapes, including nanowires [23], hollow structures [24], dendrite-like shapes [25], nanocubes [26], and nanospheres [27].

The shape control of Pt nanoparticles is vital for improving HER performance. Different crystal planes are exposed on the surface to minimize the surface energy, which leads to different active planes. (111) and (100) facets are desirable for Pt nanoparticles [28]. Synthesis methods, including hydrothermal, solvothermal, sol–gel, and electrochemical deposition methods, are widely reported for HER electrocatalyst fabrication [29]. As shown by transmission electron microscopic (TEM) images in Fig. 4A.5, Pt nanoparticles with cuboctahedra, spheres, tetrapod, truncated cubs, stars, and dendrite-like shapes are presented [30]. The changing amounts of precursors, reaction temperature, surface ligands, and nucleation processes will produce different shapes due to the different nucleation rates and growth orientation. By tuning the shapes, the specific surface areas can be increased, along with electrocatalytic sites, increasing HER performances.

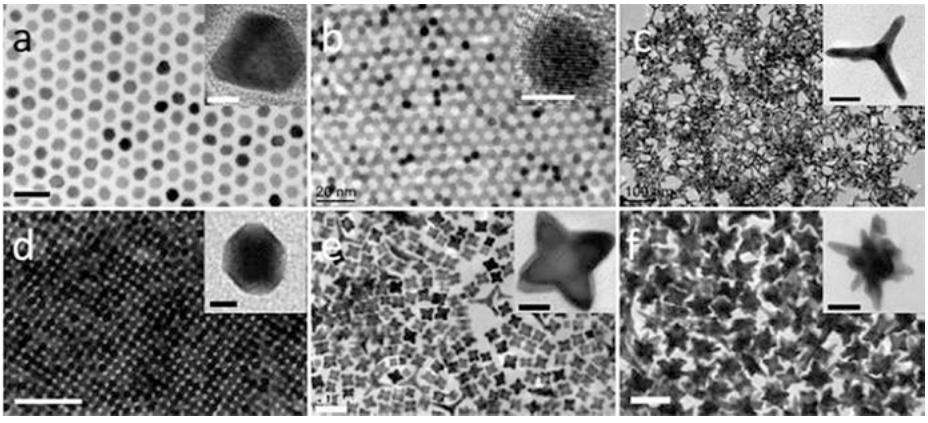

Fig. 4A.5: TEM images of (a) Pt cuboctahedra, (b) Pt spheres, (c) Pt tetrapods, (d) Pt truncated cubes, (e) Pt stars (octapods), (f) Pt multipods. Scale bars: (a, b) 20 nm, (c) 100 nm, (d, f) 50 nm; insets of (a, b, d) 5 nm; insets of (c, f) 20 nm; and inset of (e) 10 nm [30] (Copyright 2013, American Chemical Society).

Besides modifying shapes for noble nanoparticles, alloy nanoparticles are popular to achieve synergistic effects, which further improve the HER efficiency and stability of electrocatalysts compared with single-component noble-metal ones. The reaction is usually controlled by mixing two or several metal precursors to obtain alloy nanoparticles. Under different solvents, temperatures, and surfactants based on

single-metal electrocatalysts, noble metals will be simultaneously reduced, and the ratio between metals can be controlled simply by adjusting the precursors.

Pt_2Pd alloy nanoparticles were synthesized through a one-step method [31]. Platinum phthalocyanine, palladium phthalocyanine, 2, 2-dipyridylacetyene, and graphene were added into a Teflon-lined autoclave and hydrothermally treated. Finally, the Pt_2Pd nanoparticles were embedded in N-doped carbon materials and shown to act as efficient HER electrocatalysts, as shown in Fig. 4A.6. The TEM image shows that individual Pt_2Pd alloy nanoparticles are hosted within the carbon materials. The high-resolution TEM (HRTEM) presents the lattice space of 0.225 nm, corresponding to the Pt(111) plane. The ratio between Pt and Pd is 2:1 according to the line-scanning image across an alloy nanoparticle. The energy-dispersive X-ray spectroscopy (EDS) mapping images confirm the chemical composition of the alloy nanoparticle.

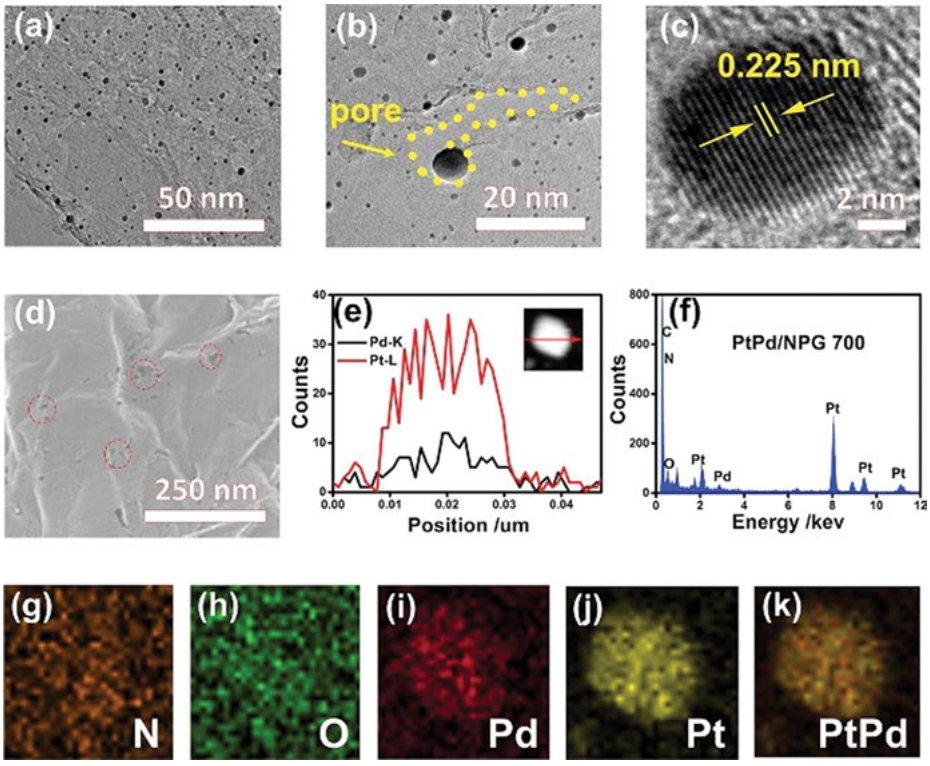

Fig. 4A.6: (a, b) TEM images of Pt_2Pd/NPG 700. (c) HRTEM image. (d) SEM image of Pt_2Pd/NPG 700. (e) Line-scanning profile across a Pt_2Pd nanoparticle, as indicated in the inset of (e). (f) EDX pattern of Pt_2Pd/NPG 700 catalyst. (g–k) EDS elemental mapping of N, O, Pd, Pt, and Pt_2Pd alloy, respectively [31] (Copyright 2017, Elsevier).

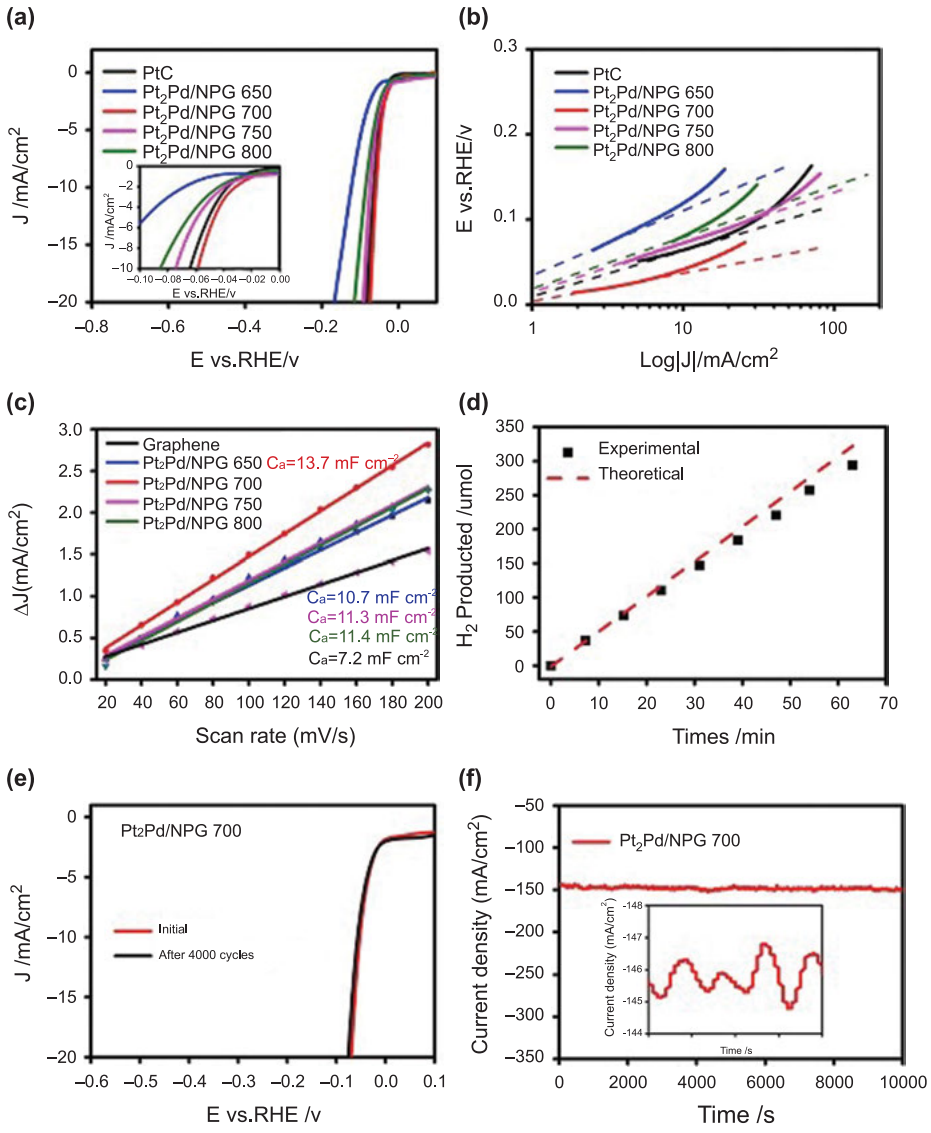

Fig. 4A.7: (a) HER performance in 0.5 M H_2SO_4. (b) Tafel plots and (c) double-layer capacitances (C_{dl}) for Pt_2Pd/NPG electrocatalysts treated with different temperatures. (d) Faradic efficiency of PtPd/NPG 700 catalysts. (e) Initial and 4,000th LSV curves of Pt_2Pd/NPG 700. (f) Time dependence of current density for Pt_2Pd/NPG 700 under a static overpotential of 140 mV. The inset shows an enlarged image [31] (Copyright 2017, Elsevier).

The HER performance was evaluated in 0.5 M H_2SO_4, as shown in Fig. 4A.7. Pt_2Pd nanoparticles annealed at different temperatures show remarkable performance, and Pt_2Pd/NPG 700 exhibits superior performance, even better than commercial Pt/C

materials. The lowest is overpotential (η_{10}) at the current density of –10 mA/cm^2 for Pt_2Pd/NPG 700. The Tafel slopes and electrochemical double-layer capacitance (C_{dl}) are illustrated in Fig. 4A.7b and c, which reflect the electrochemical active surface area (ECSA). Hydrogen production is consistent with the theoretical simulation. Additionally, the durability was verified from 4,000 linear sweep voltammetry (LSV) cycles under long-term continuous applied potential. Pt_2Pd alloy nanoparticles embedded in graphene provide a synergistic effect on interfaces and facilitate the HER reaction.

Additionally, non-noble metals can be introduced to noble-metal electrocatalysts to simultaneously lower usage and tune the electrical property. The triple metal alloy nanowires were fabricated with S-doping through reduction methods. TEM and EDS elemental mapping images are shown in Fig. 4A.8. Firstly, AuPb nanowires were fabricated through reduction methods in an aqueous solution. Then the platinum source was added and reduced on AuPb nanowires to form AuPbPt alloy nanowires [32]. The lattice fringes in HRTEM are 0.235 and 0.234 nm, corresponding to Au's (111) plane and the intermetallic PbPt, respectively. The high-angle annular dark-field scanning TEM (HAADF-STEM) and the corresponding EDS mapping images illustrate the composition of Au, Pt, and Pb in the alloy nanowires.

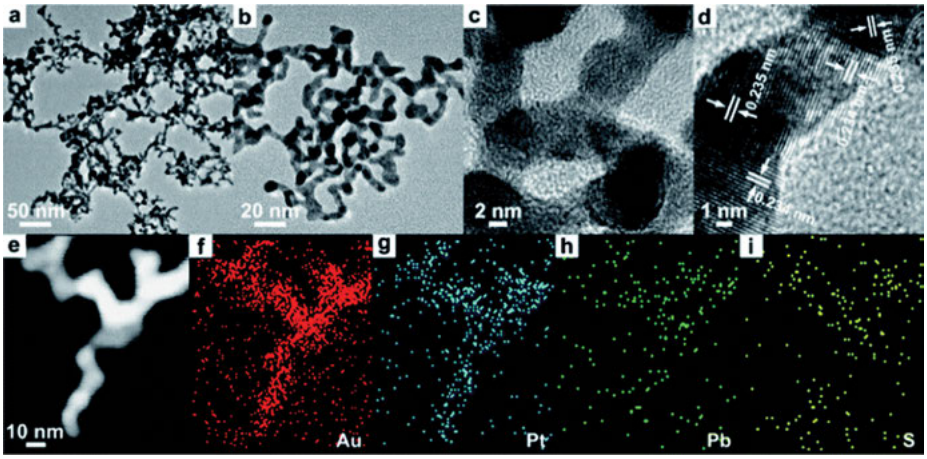

Fig. 4A.8: (a, b) TEM images and (c, d) HRTEM images of S-doped AuPbPt alloy NWs. (e) HAADF-STEM image and the corresponding EDS mapping images of (f) Au, (g) Pt, (h) Pb, and (i) S [32] (Copyright 2013, Royal Society of Chemistry).

The HER performance in acidic electrolytes is much better than commercial Pt/C electrocatalysts, as shown in Fig. 4A.9. The mass activity is 12.3 times (at –0.05 V vs. RHE) and 3.4 times (at –0.07 V vs. RHE) higher than the commercial Pt/C materials. The Tafel slope of the AuPbPt alloy is 17.7 mV/dec, lower than that of Pt/C, indicating that the Volmer–Tafel process is the determining step. After 5,000 cycles of cyclic voltammetry tests, the performance has almost no decrease, showing remarkable stability.

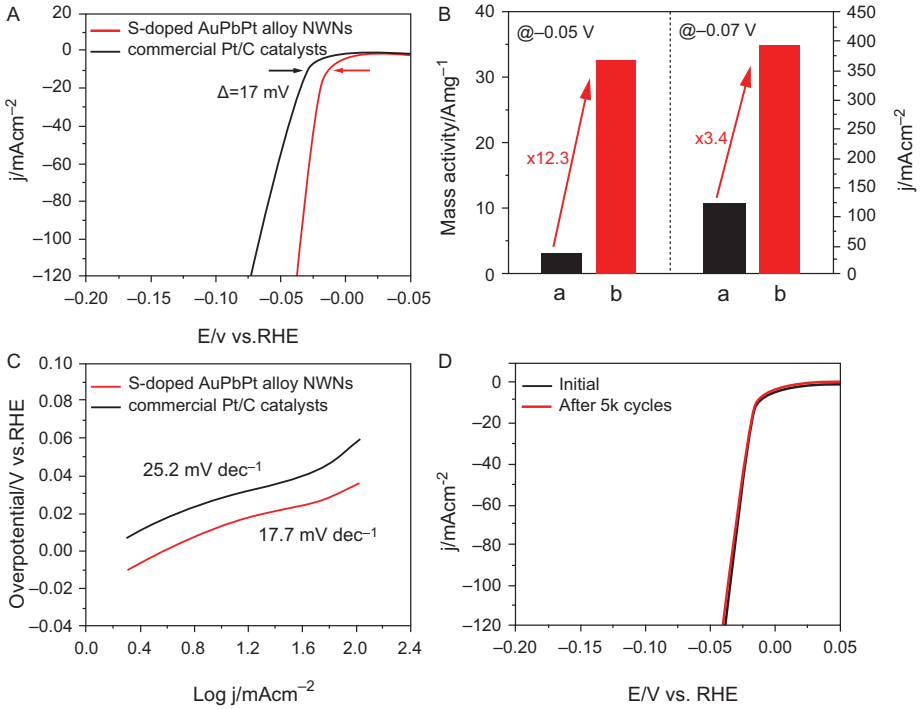

Fig. 4A.9: (a) HER performance of S-doped AuPbPt alloy NWs and commercial Pt/C catalysts in N_2-saturated 0.5 M H_2SO_4 solution. (b) Mass activity (at 0.05 V vs. RHE) and current density (at 0.07 V vs. RHE) of the S-doped AuPbPt alloy NWs and commercial Pt/C catalysts. (c) Tafel plots of S-doped AuPbPt alloy NWs and commercial Pt/C catalysts. (d) LSV curves of Si-doped AuPbPt alloy NWs before and after 5,000 cycles of the accelerated durability test in a 0.5 M H_2SO_4 solution [32] (Copyright 2013, Royal Society of Chemistry).

Single-atom catalysts (SACs) are realized to reach a maximum utilization rate of noble metals near 100 %. Methods that utilize the noble metal at an atomic level can substantially decrease the cost. Various methods, including photochemical reaction, atomic-layer deposition, and thermal reduction, have been developed [33]. Meantime, the HER performance is superior to noble-metal nanoparticles with the same noble-metal loading. Single atoms of noble metals anchored on substrates have been developed very quickly over recent years [34].

For SACs, the surface coordination status of the metal atom will greatly affect their electronic structures, which subsequently influence the catalytic activity. The substrates supporting single atoms are quite significant, such as graphene, C_3N_4, and MoS_2, and are widely explored [35].

A stable substrate and adjustable coordination conditions were studied to understand Pt single-atom electrocatalyst. Graphdiyne (GDY) was chosen as the substrate, and the atomically dispersed Pt atoms were loaded on GDY through a wet-chemical

strategy. The as-prepared single-atom Pt can be observed from TEM images, as shown in Fig. 4A.10. The Pt-GDY1 and Pt-GDY2 samples are under different temperature treatments. The Pt-GDY1 was synthesized at room temperature while Pt-GDY2 was further treated at 200 °C from Pt-GDY1, making Pt in Pt-GDY2 a more positive valence state than in Pt-GDY1 [36].

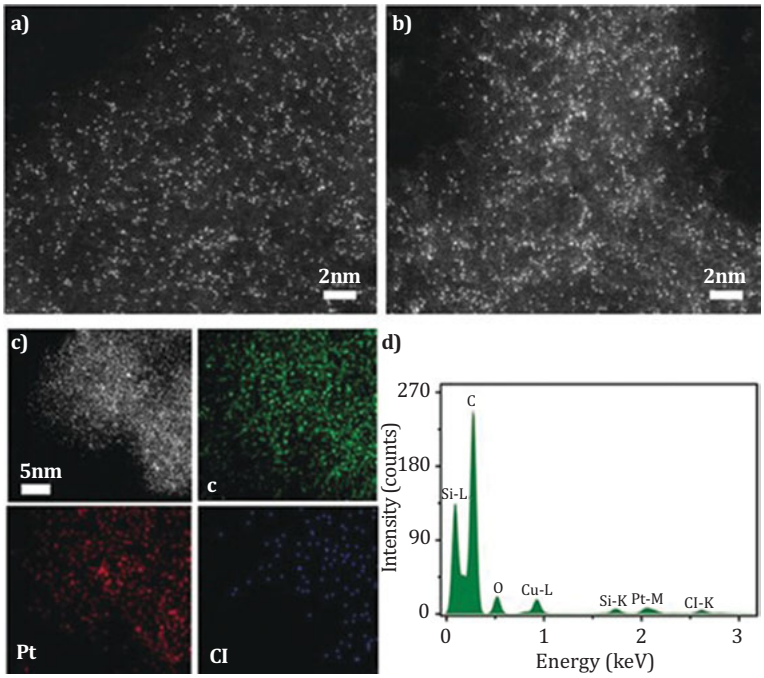

Fig. 4A.10: Atomic-resolution HAADF-STEM images of (a) Pt-GDY1 and (b) Pt-GDY2. (c) Elemental mapping of Pt-GDY2. (d) The EDS analysis of Pt-GDY2 [36] (Copyright 2018, John Wiley and Sons).

Figure 4A.10 shows the HAADF-STEM image of Pt single atom on GDY. The individual Pt atoms are observed, and the EDS mapping confirms the elemental composition. With the successful Pt loading on GDY, the HER performance of Pt-GDY2 shows much better HER performance than commercial Pt/C. The mass activity is 23.64 times that of Pt/C, illustrating the efficient Pt usage for electrocatalysis, as shown in Fig. 4A.11. The Tafel slope indicates that Volmer–Heyrovsky is the determining step. The 1,000 cycles of LSV tests confirm the excellent stability of SACs. The isolated Pt atoms were anchored on GDY by the coordination interactions of the C-Pt-Cl_4 group, and the higher unoccupied density of states of Pt 5d orbital makes Pt-GDY2 more efficient for HER.

In addition, Pt, Ru, Ir, and Pd were studied for HER with the development of SACs [37, 38]. With the development of noble-metal materials, from shape modification and alloy composition to single-atom incorporation, the HER performance increases with the decrease in the amount of noble-metal loading, making them promising for future

HER applications. Noble-metal-based electrocatalysts lead the best-in-class HER performance. The latest HER performance is listed in Tab. 4A.1.

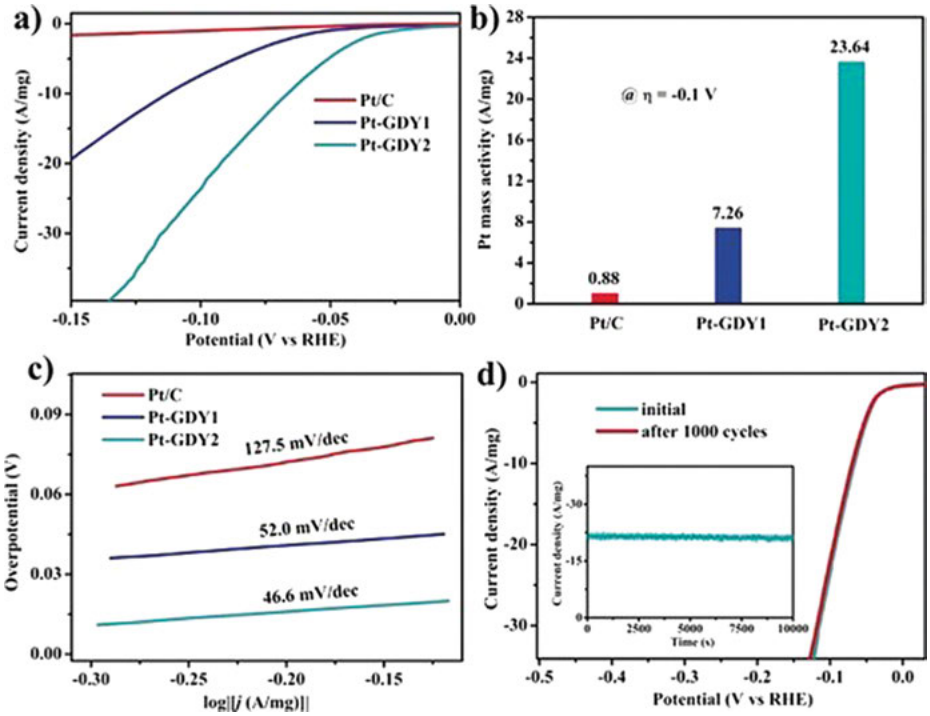

Fig. 4A.11: (a) LSV curves of Pt-GDY1, Pt-GDY2, and commercial Pt/C in 0.5 M H_2SO_4 solution. (b) The HER mass activity at $\eta = 0.1$ V for Pt/C, Pt-GDY1, and Pt-GDY2. (c) Tafel plots of Pt/C, Pt-GDY1, and Pt-GDY2. (d) The LSV curves of Pt-GDY2 at initial and after 1,000 cycles with a scan rate of 5 mV/s. The inset shows the time-dependent current density curve at 95 mV versus RHE [36] (Copyright 2018, John Wiley and Sons).

4A.3.2 Transition-metal-based electrocatalyst

Transition metals outside the Pt, Ir, Pd, and Ru groups are promising alternatives due to their abundance and occasional excellent HER performance. First-row transition metals have been introduced into noble-metal electrocatalysts to replace part of the noble metals and form alloy nanoparticles, Pt–Co [47] and Pt–Ni [48], that show impressive HER performances. Among transition-metal-based electrocatalysts, transition-metal phosphides (TMPs) have gained intensive attention due to their adjustable compositions and structures, tunable electronic properties, and remarkable electrical conductivities, which present comparable HER performance with commercial Pt/C [49].

Tab. 4A.1: Comparison of latest noble-metal-based electrocatalysts on HER performance.

Electrocatalyst	Overpotential η_{10} (mV)	Tafel slope (mV/dec)	Electrolyte	Reference
Pt dendrite	15	31	0.5 M H_2SO_4	[39]
Ru nanodot	14	32.5	1 M PBS	[40]
Pt cluster	35	61	1 M PBS	[25]
Pt/Ru nanocrystal	22	19	1 M KOH	[41]
Ru/Pd nanowire	11	50	1 M KOH	[42]
Pt/Ni nanowire	13	29	1 M KOH	[43]
Pt_{SA}-MWCNTS	43.9	30	0.5 M H_2SO_4	[44]
Ru_{SA}-N-$Ti_3C_2T_X$	27	29	1 M KOH	[45]
Pt_{SA}-CN	13	34	1 M $HClO_4$	[46]

More than 100 bimetallic phosphides have been studied [50], which provide large possibilities for tuning the ratios and compositions of TMPs and their electronic structures. The phosphorization process can successfully introduce P into transition-metal electrocatalysts, forming P-metal bonds. The comparatively higher electronegativity of P in the TMPs connected with metal atoms leads to a proton-acceptor process for promoting HER performance [50]. CoP [51], NiP [52], and bimetallic CoP/Ni_2P [53] and CoP/Co_2P [54] have been explored, and their HER performances are remarkable.

TMPs are often fabricated on substrates as self-standing electrodes. The vertical CoP nanoarray was fabricated through three steps. Firstly, the CoCH nanorods were formed from the hydrothermal method on Ti foil and then immersed in 2-methylimidazole to grow the ZIF-67 shell. Finally, CoP/NPC/TF was acquired through a phosphatization process at 400 °C, as shown in Fig. 4A.12.

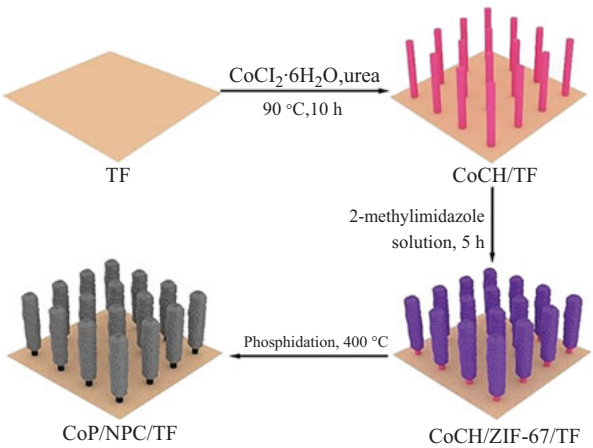

Fig. 4A.12: Schematic illustration of the synthetic process of the CoP/NPC/TF [55] (Copyright 2019, John Wiley and Sons).

The as-prepared CoP nanoarray performed in 0.5 M H_2SO_4 is shown in Fig. 4A.13. The optimized CoP/NPC/TF electrode shows comparable HER performance with commercial Pt/C. The Tafel slopes and overpotentials (η_{10}) are close to Pt/C; double-layer capacitance reflects the ECSA for the modified materials. The LSV cycling and long-term durability tests indicate its superb stability [55].

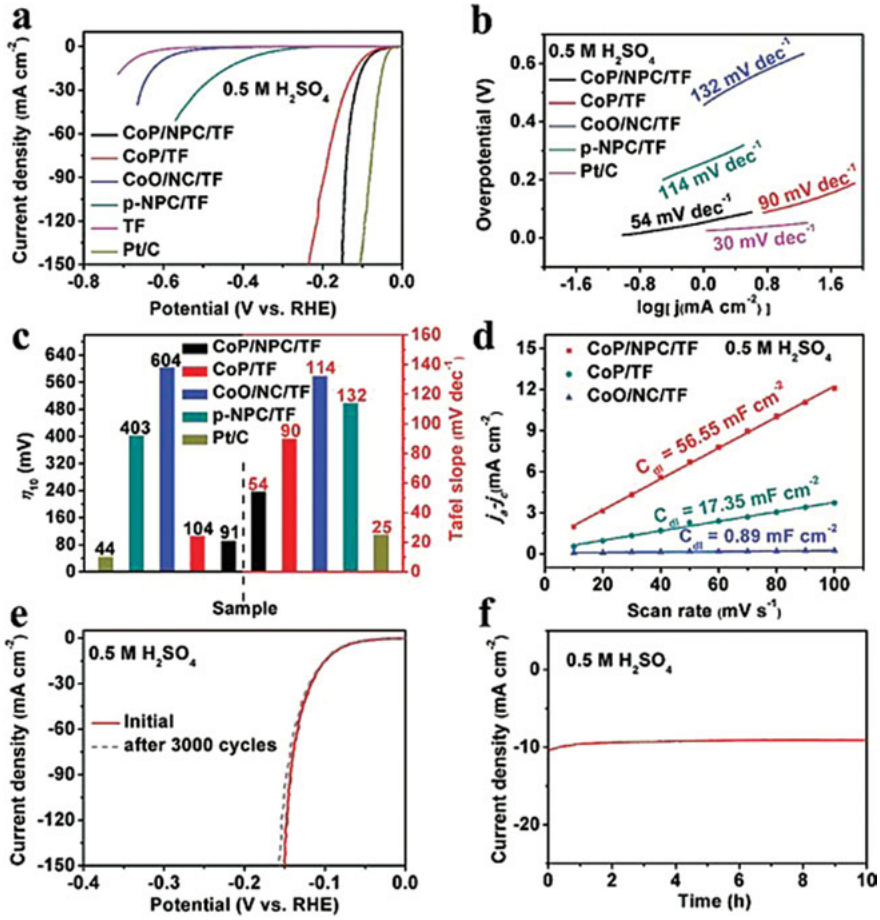

Fig. 4A.13: (a) HER performance and (b) Tafel plots of CoP/NPC/TF and other references with a scan rate of 2 mV/s in 0.5 M H_2SO_4. (c) The comparison of overpotential at 10 mA/cm^2 and Tafel slopes of CoP/NPC/TF and other references. (d) Double-layer capacitances (C_{dl}) at −0.15 V versus RHE as a function of scan rate for CoP/NPC/TF, CoP/TF, and CoO/NC/TF. (e) LSV curves of CoP/NPC/TF before and after 3,000 cycles. (f) Time-dependent current density curve of CoP/NPC/TF under a constant overpotential of 103 mV for 10 h [55] (Copyright 2019, John Wiley and Sons).

Transition-metal-based electrocatalysts have flourished, and some of the latest electrocatalysts are listed in Tab. 4A.2.

Tab. 4A.2: Comparison of latest transition-metal-based electrocatalyst on HER performance.

Electrocatalyst	Overpotential η_{10} (mV)	Tafel slope (mV/dec)	Electrolyte	Reference
Mn-Ni	80	68	1 M KOH	[56]
Co_{SA}/C	230	99	0.5 M H_2SO_4	[57]
Ni_{SA}-MoS_2	98	74	1 M KOH	[58]
B-CoP/CNT	79	80	1 M PBS	[59]
NiO-NiP	76	98	1 M KOH	[52]
CoP/Co_2P	103	61.2	1 M KOH	[60]
NiCoP/CoP	73	91.3	1 M KOH	[61]
CoP/CoMoP	34	33	1 M KOH	[62]

4A.3.3 Metal-free electrocatalyst

Noble-metal-based materials are regarded as the most efficient HER electrocatalysts. However, the limited abundance and high cost restrict future application, and thus developing electrocatalysts with earth-abundance materials is promising. Metal-free electrocatalysts are considered potentially efficient HER electrocatalysts, mostly carbon-based materials. However, the pristine carbon materials have limited and poor electrocatalytic activity. To increase the HER performance of carbon materials, a surface chemical environment is required by doping heteroatoms, such as N, S, and P [63]. The dopants in carbon materials lead to physical- and chemical-tuning properties, increasing the electrocatalytic HER performance.

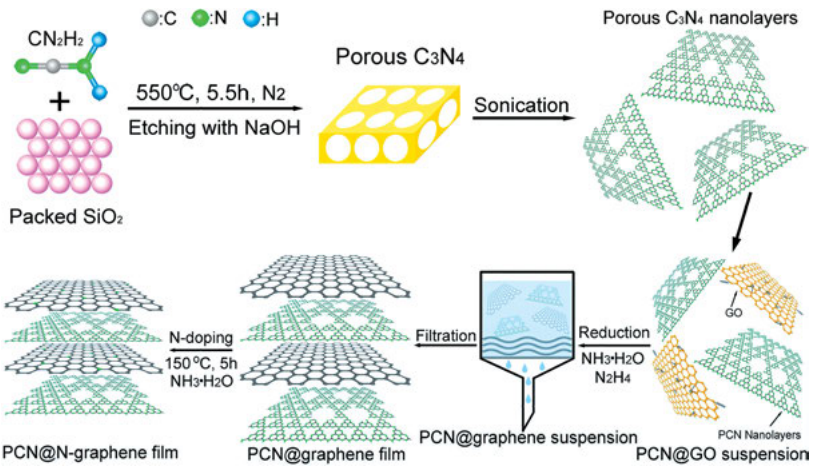

Fig. 4A.14: Schematic illustration of the fabrication process of PCN@N-graphene film [64] (Copyright 2015, American Chemical Society).

Nitrogen-doped carbon is a widely explored material in metal-free electrocatalysts. When nitrogen is introduced into the carbon, properties such as electronic structures and electrocatalytic activities are improved. The HER performance is based on the amount of N dopants. Moreover, the efficient N-doped carbon electrodes also depend on the surface structure. As shown in Fig. 4A.14, porous C_3N_4 is integrated with N-doped graphene film to form the catalyst without substrate [64]. The hierarchical structure, large specific surface area, and highly exposed electrocatalytic sites enable the electrode to achieve fabulous HER performance with a low onset overpotential and excellent stability, as shown in Fig. 4A.15.

The HER performance is much closer to Pt/C with N doping in graphene and annealing treatment, verified by the low Tafel slopes and overpotentials (η_{10}). The charge transfer resistance (R_{ct}) is indicated in Fig. 4A.15d, which is related to the kinetics. The lower value of R_{ct} presents the fast reaction during HER. The 5,000 cycles of LSV tests activate the as-prepared materials, resulting in better performance. Meantime, the stability is also remarkable for long-term tests.

However, due to the intrinsic properties of carbon materials, the efficient HER performance is still a challenge, which could not hinder its advantages of stability, low cost, and recycling properties. More importantly, double or triple hetero-atom doping was further explored, such as N and S and N and P doping in carbon material [63]. The metal-free electrocatalyst is another way to realize stable and efficient hydrogen production. The latest HER performance of metal-free-based electrocatalyst is listed in Tab. 4A.3.

4A.4 Hydrogen storage

The utilization of hydrogen directly from water splitting is limited, and thus hydrogen storage and transport are quite significant. Developing a safe, cost-effective method for hydrogen storage is still a challenge. Nowadays, compression, liquid, chemical, and physical storage are the four main storage methods that are widely explored [70].

4A.4.1 Compression storage

Hydrogen can be stored as a compressed gas in high-pressure tanks, and it can be transported through pipelines like natural gas. The compression storage method is simple and can increase the energy density for hydrogen but requires high-level storage equipment.

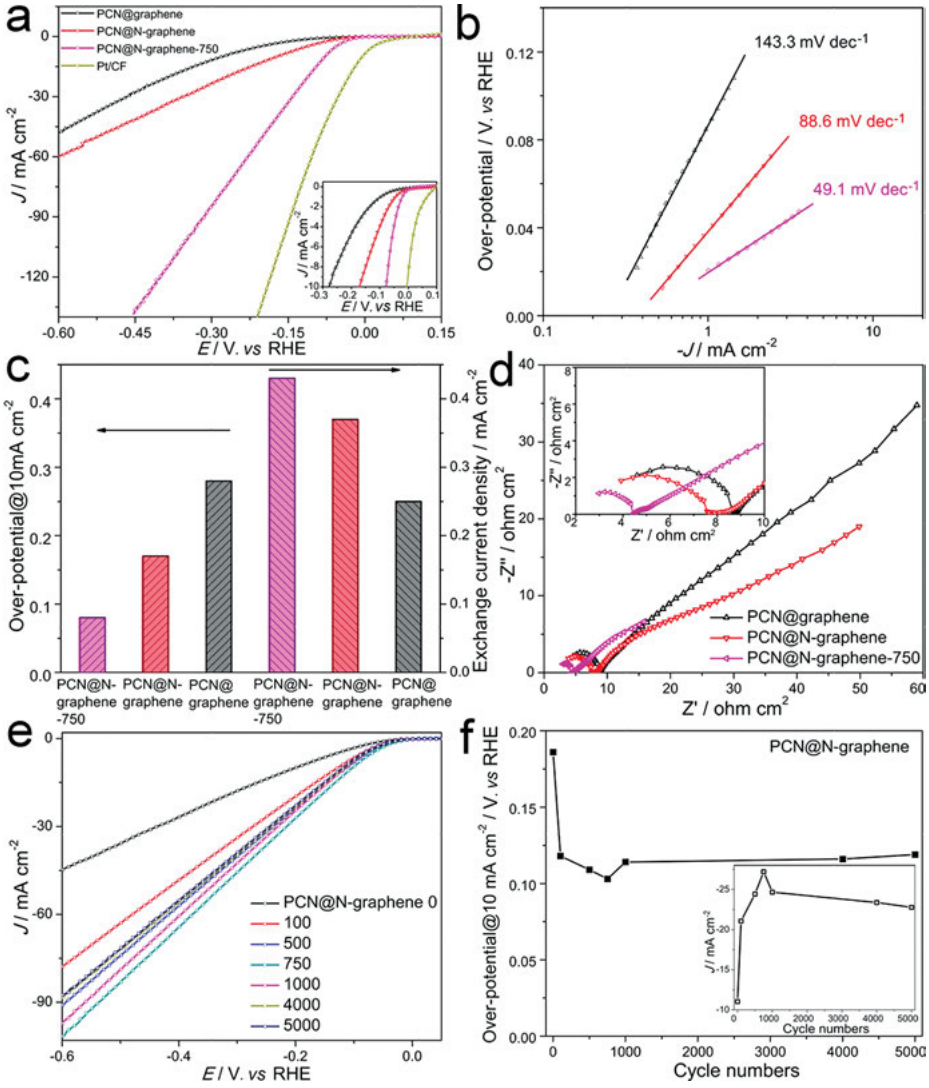

Fig. 4A.15: (a) LSV curves (inset shows LSV curves with the current density below 10 mA/cm^2). (b) Tafel plots and (c) overpotential@10 mA/cm^2 versus RHE (left) and exchange current density (right). (d) Electrochemical impedance spectra at 0.2 V versus RHE of PCN@graphene, PCN@N-graphene, and PCN@N-graphene-750 films. (e) The polarization curves after different cyclic voltammetry (CV) cycles. (f) Required overpotential@10 mA/cm^2 versus RHE plotted as CV cycle numbers of PCN@N-graphene film (inset is the current density@0.2 V versus RHE [64] (Copyright 2015, American Chemical Society).

Tab. 4A.3: Comparison of latest metal-free electrocatalyst on HER performance.

Electrocatalyst	Overpotential η_{10} (mV)	Tafel slope (mV/dec)	Electrolyte	Reference
g-C_3N_4/N-graphene	80	49.1	0.5 M H_2SO_4	[64]
N, S-graphene	130	80.5	0.5 M H_2SO_4	[65]
N, P-graphene	420	91	0.5 M H_2SO_4	[66]
N, P-carbon	204	58	0.5 M H_2SO_4	[67]
g-C_3N_4 nanoribbons/ graphene	207	54	0.5 M H_2SO_4	[68]
TpPAM	250	106	0.5 M H_2SO_4	[69]

4A.4.2 Liquid storage

Liquid hydrogen storage is a normal storage method, but the high pressure required for liquid hydrogen storage leads to many challenges for the fabrication of storage equipment. Meantime, the low temperature reaching 21 K is also quite strict. The efficient load and release processes are also difficult.

4A.4.3 Chemical storage

Nowadays, more and more researchers focus on hydrogen storage materials to realize the fast adsorption and release of hydrogen in a favorable environment. The chemical storage materials involve chemical bond forming and breaking. Under certain temperatures and pressures, hydrogen can be adsorbed and generated through a chemical reaction in many materials, including metal hydrides ($LiBH_4$, $NaAlH_4$, $NaBH_4$, etc.) [71, 72].

4A.4.4 Physical storage

Molecular hydrogen can get absorbed on the surface of some materials, which are called physical storage materials. Physisorption only involves physical adsorption and desorption, which requires high pressure for large amounts of storage, unlike chemical storage materials. The most studied materials are carbon materials (graphene and nanotubes) [73], organic metal frameworks [74], and covalent organic frameworks [75].

With the rapid development of electrocatalytic water splitting and advanced materials, hydrogen storage technology and materials are pursued as an essential foundation for renewable energy systems. The comparison among different storage methods is shown in Tab. 4A.4.

Tab. 4A.4: Comparison of four hydrogen storage methods.

	Chemical storage	**Physical storage**	**Compressed storage**	**Liquid storage**
Interaction	Chemical bonding	Van der Waals	Compression	High-pressure compression
Energy requirement	Large	Low	Large	Large
Transfer rate	Slow	Fast	Fast	Fast
Temperature (K)	400–600	Varies	273	21
Volumetric capacity (kg/m^3)	~150	~20	~30	~70
Advantage	High storage density Feature selectivity	Fast reversible process Low storage cost	Lightweight Easy storage technology	Long-term storage Highest energy density
Limitation	The slow activation process Impurity absorption High temperature Slow-release kinetic	Weak interaction High pressure Volumetrically inefficient	High-pressure tanks Volumetrically inefficient	High-pressure tanks Energy loss High pressure Low temperature

4A.5 Summary

With the fast development of hydrogen energy, future energy systems will be more adjustable, reducing pollution and optimizing the energy network caused by the uneven consumption and distribution of fossil fuels. Electrochemical water splitting has great potential due to its easy fabrication processes, pure hydrogen collection, and safety steps. Meanwhile, the studies of numerous electrocatalysts, working mechanisms, and hydrogen storage materials lead to more and more efficient hydrogen production and storage, which shows promising future applications in the whole clean energy system.

References

[1] Barreto, L., Makihira, A. & Riahi, K. (2003). The hydrogen economy in the twenty-first century: a sustainable development scenario. International Journal of Hydrogen Energy, 28, 267–284.

[2] Chen, G., Li, J., Li, K., Lin, F., Tian, W., Che, L., Yan, B., Ma, W. & Song, Y. (2020). Nitrogen, sulfur, and chlorine-containing pollutants are releasing characteristics during pyrolysis and combustion of oily sludge. Fuel, 273, 117772.
[3] Gielen, D., Boshell, F., Saygin, D., Bazilian, M. D., Wagner, N. & Gorini, R. (2019). The role of renewable energy in the global energy transformation. Energy Strategy Reviews, 24, 38–50.
[4] Neumann, A., Sorge, L., von Hirschhausen, C. & Wealer, B. (2020). Democratic quality, and nuclear power: reviewing the global determinants for introducing nuclear energy in 166 countries. Energy Research & Social Science, 63, 101389.
[5] Esposito, D. V. (2017). Membraneless electrolyzers for low-cost hydrogen production in a renewable energy future. Joule, 1, 651–658.
[6] Mayyas, A., Wei, M. & Levis, G. (2020). Hydrogen as a long-term, large-scale energy storage solution when coupled with renewable energy sources or grids with dynamic electricity pricing schemes. International Journal of Hydrogen Energy, 45, 16311–16325.
[7] Song, Y., Zhang, C., Ling, C.-Y., Han, M., Yong, R.-Y., Sun, D. & Chen, J. (2020). Review on current research of materials, fabrication, and application for bipolar plate in proton exchange membrane fuel cell. International Journal of Hydrogen Energy, 45, 29832–29847.
[8] Zhang, G. & Jiao, K. (2018). Multi-phase models for water and thermal management of proton exchange membrane fuel cell: a review. Journal of Power Sources, 391, 120–133.
[9] Hassanpouryouzband, A., Joonaki, E., Edlmann, K., Heinemann, N. & Yang, J. (2020). Thermodynamic and transport properties of hydrogen-containing streams. Scientific Data, 7, 222.
[10] Xu, R., Chou, L.-C. & Zhang, W.-H. (2019). The effect of CO_2 emissions and economic performance on hydrogen-based renewable production in 35 European Countries. International Journal of Hydrogen Energy, 44, 29418–29425.
[11] Changizian, S., Ahmadi, P., Raeesi, M. & Javani, N. (2020). Performance optimization of hybrid hydrogen fuel cell electric vehicles in real driving cycles. International Journal of Hydrogen Energy, 45, 35180–35197.
[12] Sazali, N. (2020). Emerging technologies by hydrogen: a review. International Journal of Hydrogen Energy, 45, 18753–18771.
[13] Cai, L., He, T., Xiang, Y. & Guan, Y. (2020). Study on the reaction pathways of steam methane reforming for H_2 production. energy, 207, 118296.
[14] Ji, G., Zhao, M. & Wang, G. (2018). Computational fluid dynamic simulation of a sorption-enhanced palladium membrane reactor for enhancing hydrogen production from methane steam reforming. energy, 147, 884–895.
[15] Filippov, S. P. & Yaroslavtsev, A. B. (2021). Hydrogen energy: development prospects and materials. Russian Chemical Reviews, 90, 627–643.
[16] Ganguly, P., Harb, M., Cao, Z., Cavallo, L., Breen, A., Dervin, S., Dionysiou, D. D. & Pillai, S. C. (2019). 2D nanomaterials for photocatalytic hydrogen production. ACS Energy Letters, 4, 1687–1709.
[17] Soloveichik, G. (2019). Electrochemical synthesis of ammonia as a potential alternative to the Haber–Bosch process. Nature Catalysis, 2, 377–380.
[18] Chen, S., Li, M., Gao, M., Jin, J., van Spronsen, M. A., Salmeron, M. B. & Yang, P. (2020). High-performance Pt-Co nanoframes for fuel-cell electrocatalysis. Nano Letters, 20, 1974–1979.
[19] Ďurovič, M., Hnát, J. & Bouzek, K. (2021). Electrocatalysts for the hydrogen evolution reaction in alkaline and neutral media. A comparative review. Journal of Power Sources, 493, 229708.
[20] Nørskov, J. K., Bligaard, T., Logadottir, A., Kitchin, J. R., Chen, J. G., Pandelov, S. & Stimming, U. (2005). Trends in the exchange current for hydrogen evolution. Journal of the Electrochemical Society, 152, J23.

[21] Cai, J., Javed, R., Ye, D., Zhao, H. & Zhang, J. (2020). Recent progress in noble metal nanocluster and single-atom electrocatalysts for the hydrogen evolution reaction. Journal of Materials Chemistry A, 8, 22467–22487.
[22] Zou, X. & Zhang, Y. (2015). Noble metal-free hydrogen evolution catalysts for water splitting. Chemical Society Reviews, 44, 5148–5180.
[23] Li, H., Wu, X., Tao, X., Lu, Y. & Wang, Y. (2020). Direct synthesis of ultrathin Pt nanowire arrays as catalysts for methanol oxidation. Small, 16, 2001135.
[24] Ge, C., Wu, R., Chong, Y., Fang, G., Jiang, X., Pan, Y., Chen, C. & Yin, -J.-J. (2018). Synthesis of Pt hollow nanodendrites with enhanced peroxidase-like activity against bacterial infections: implication for wound healing. Advanced Functional Materials, 28, 1801484.
[25] Tan, Y., Xie, R., Zhao, S., Lu, X., Liu, L., Zhao, F., Li, C., Jiang, H., Chai, G., Brett, D. J. L., Shearing, P. R., He, G. & Parkin, I. P. (2021). Facile fabrication of robust hydrogen evolution electrodes under high current densities via Pt@Cu interactions. Advanced Functional Materials, 31, 2105579.
[26] Darmadi, I., Stolaś, A., Östergren, I., Berke, B., Nugroho, F. A. A., Minelli, M., Lerch, S., Tanyeli, I., Lund, A., Andersson, O., Zhdanov, V. P., Liebi, M., Moth-Poulsen, K., Müller, C. & Langhammer, C. (2020). Bulk-processed Pd nanocube–poly(methyl methacrylate) nanocomposites as plasmonic plastics for hydrogen sensing. ACS Applied Nano Materials, 3, 8438–8445.
[27] Su, D. W., Dou, S. X. & Wang, G. X. (2015). Hierarchical Ru nanospheres as highly effective cathode catalysts for Li–O_2 batteries. Journal of Materials Chemistry A, 3, 18384–18388.
[28] Duan, S., Du, Z., Fan, H. & Wang, R. (2018). Nanostructure optimization of platinum-based nanomaterials for catalytic applications. Nanomaterials, 8.
[29] Zhang, L., Doyle-Davis, K. & Sun, X. (2019). Pt-based electrocatalysts with high atom utilization efficiency: from nanostructures to single atoms. Energy & Environmental Science, 12, 492–517.
[30] Kang, Y., Pyo, J. B., Ye, X., Diaz, R. E., Gordon, T. R., Stach, E. A. & Murray, C. B. (2013). Shape-controlled synthesis of Pt nanocrystals: the role of metal carbonyls. ACS Nano, 7, 645–653.
[31] Zhong, X., Qin, Y., Chen, X., Xu, W., Zhuang, G., Li, X. & Wang, J. (2017). PtPd alloy embedded in nitrogen-rich graphene nanopores: high-performance bifunctional electrocatalysts for hydrogen evolution and oxygen reduction. carbon, 114, 740–748.
[32] Zhang, X., Wang, S., Wu, C., Li, H., Cao, Y., Li, S. & Xia, H. (2020). Synthesis of S-doped AuPbPt alloy nanowire-networks as superior catalysts towards the ORR and HER. Journal of Materials Chemistry A, 8, 23906–23918.
[33] Zhang, L., Ren, Y., Liu, W., Wang, A. & Zhang, T. (2018). Single-atom catalyst: a rising star for green synthesis of fine chemicals. National Science Review, 5, 653–672.
[34] Liu, Q. & Zhang, Z. (2019). Platinum single-atom catalysts: a comparative review towards effective characterization. Catalysis Science and Technology, 9, 4821–4834.
[35] Deng, J., Li, H., Xiao, J., Tu, Y., Deng, D., Yang, H., Tian, H., Li, J., Ren, P. & Bao, X. (2015). Triggering the electrocatalytic hydrogen evolution activity of the inert two-dimensional MoS_2 surface via single-atom metal doping. Energy & Environmental Science, 8, 1594–1601.
[36] Yin, X.-P., Wang, H.-J., Tang, S.-F., Lu, X.-L., Shu, M., Si, R. & Lu, T.-B. (2018). Engineering the coordination environment of single-atom platinum anchored on graphdiyne for optimizing electrocatalytic hydrogen evolution. Angewandte Chemie International Edition, 57, 9382–9386.
[37] Lai, W.-H., Zhang, L.-F., Hua, W.-B., Indris, S., Yan, Z.-C., Hu, Z., Zhang, B., Liu, Y., Wang, L., Liu, M., Liu, R., Wang, Y.-X., Wang, J.-Z., Hu, Z., Liu, H.-K., Chou, S.-L. & Dou, S.-X. (2019). General π-electron-assisted strategy for Ir, Pt, Ru, Pd, Fe, Ni single-atom electrocatalysts with

bifunctional active sites for highly efficient water splitting. Angewandte Chemie International Edition, 58, 11868–11873.
[38] Li, C. & Baek, J.-B. (2020). Recent advances in noble metal (Pt, Ru, and Ir)-based electrocatalysts for efficient hydrogen evolution reaction. ACS Omega, 5, 31–40.
[39] Lin, L., Sun, Z., Yuan, M., He, J., Long, R., Li, H., Nan, C., Sun, G. & Ma, S. (2018). Significant enhancement of hydrogen evolution reaction performance through a shape-controlled synthesis of hierarchical dendrite-like platinum. Journal of Materials Chemistry A, 6, 8068–8077.
[40] Xu, C., Ming, M., Wang, Q., Yang, C., Fan, G., Wang, Y., Gao, D., Bi, J. & Zhang, Y. (2018). Facile synthesis of effective Ru nanoparticles on carbon by adsorption-low temperature pyrolysis strategy for hydrogen evolution. Journal of Materials Chemistry A, 6, 14380–14386.
[41] Li, Y., Pei, W., He, J., Liu, K., Qi, W., Gao, X., Zhou, S., Xie, H., Yin, K., Gao, Y., He, J., Zhao, J., Hu, J., Chan, T.-S., Li, Z., Zhang, G. & Liu, M. (2019). Hybrids of PtRu nanoclusters and black phosphorus nanosheets for highly efficient alkaline hydrogen evolution reaction. ACS Catalysis, 9, 10870–10875.
[42] Kweon, Y., Noh, S. & Shim, J. H. (2021). Low content Ru-incorporated Pd nanowires for bifunctional electrocatalysis. RSC Advances, 11, 28775–28784.
[43] Xie, Y., Cai, J., Wu, Y., Zang, Y., Zheng, X., Ye, J., Cui, P., Niu, S., Liu, Y., Zhu, J., Liu, X., Wang, G. & Qian, Y. (2019). Boosting water dissociation kinetics on Pt–Ni nanowires by N-induced orbital tuning. Advanced Materials, 31, 1807780.
[44] Ji, J., Zhang, Y., Tang, L., Liu, C., Gao, X., Sun, M., Zheng, J., Ling, M., Liang, C. & Lin, Z. (2019). Platinum single-atom and cluster anchored on functionalized MWCNTs with ultrahigh mass efficiency for electrocatalytic hydrogen evolution. Nano Energy, 63, 103849.
[45] Liu, H., Hu, Z., Liu, Q., Sun, P., Wang, Y., Chou, S., Hu, Z. & Zhang, Z. (2020). Single-atom Ru anchored in nitrogen-doped MXene (Ti_3C_2Tx) as an efficient catalyst for the hydrogen evolution reaction at all pH values. Journal of Materials Chemistry A, 8, 24710–24717.
[46] Chen, S., Lv, C., Liu, L., Li, M., Liu, J., Ma, J., Hao, P., Wang, X., Ding, W., Xie, M. & Guo, X. (2021). High-temperature treatment to engineer the single-atom Pt coordination environment towards highly efficient hydrogen evolution. Journal of Energy Chemistry, 59, 212–219.
[47] Zhang, S. L., Lu, X. F., Wu, Z.-P., Luan, D. & Lou, X. W. (2021). Engineering Platinum–Cobalt Nano-alloys in Porous Nitrogen-Doped Carbon Nanotubes for Highly Efficient Electrocatalytic Hydrogen Evolution. Angewandte Chemie International Edition, 60, 19068–19073.
[48] Zhang, C., Chen, B., Mei, D. & Liang, X. (2019). The OH^--driven synthesis of Pt–Ni nanocatalysts with atomic segregation for alkaline hydrogen evolution reaction. Journal of Materials Chemistry A, 7, 5475–5481.
[49] Shi, Y. & Zhang, B. (2016). Recent advances in transition metal phosphide nanomaterials: synthesis and applications in hydrogen evolution reaction. Chemical Society Reviews, 45, 1529–1541.
[50] Weng, C.-C., Ren, J.-T. & Yuan, Z.-Y. (2020). Transition metal phosphide-based materials for efficient electrochemical hydrogen evolution: a critical review. ChemSusChem, 13, 3357–3375.
[51] Yang, X., Lu, A.-Y., Zhu, Y., Hedhili, M. N., Min, S., Huang, K.-W., Han, Y. & Li, L.-J. (2015). CoP nanosheet assembly, grew on carbon cloth: a highly efficient electrocatalyst for hydrogen generation. Nano Energy, 15, 634–641.
[52] Sun, C., Wang, H., Ren, J., Wang, X. & Wang, R. (2021). Inserting ultrafine NiO nanoparticles into amorphous NiP sheets by in situ phase reconstruction for high-stability of the HER catalysts. Nanoscale, 13, 13703–13708.

[53] Feng, T., Wang, F., Xu, Y., Chang, M., Jin, X., Yulin, Z., Piao, J. & Lei, J. (2021). CoP/Ni_2P heteronanoparticles integrated with atomic Co/Ni dual sites for enhanced electrocatalytic performance toward hydrogen evolution. International Journal of Hydrogen Energy, 46, 8431–8443.
[54] Chen, T., Ye, B., Dai, H., Qin, S., Zhang, Y. & Yang, Q. (2021). Ni-doped CoP/Co_2P nanospheres as highly efficient and stable hydrogen evolution catalysts in acidic and alkaline mediums. Journal of Solid State Chemistry, 301, 122299.
[55] Huang, X., Xu, X., Li, C., Wu, D., Cheng, D. & Cao, D. (2019). Vertical CoP Nanoarray Wrapped by N, P-Doped Carbon for Hydrogen Evolution Reaction in Both Acidic and Alkaline Conditions. Advanced Energy Materials, 9, 1803970.
[56] Shao, Q., Wang, Y., Yang, S., Lu, K., Zhang, Y., Tang, C., Song, J., Feng, Y., Xiong, L., Peng, Y., Li, Y., Xin, H. L. & Huang, X. (2018). Stabilizing and Activating Metastable Nickel Nanocrystals for Highly Efficient Hydrogen Evolution Electrocatalysis. ACS Nano, 12, 11625–11631.
[57] Hossain, M. D., Liu, Z., Zhuang, M., Yan, X., Xu, G.-L., Gadre, C. A., Tyagi, A., Abidi, I. H., Sun, C.-J., Wong, H., Guda, A., Hao, Y., Pan, X., Amine, K. & Luo, Z. (2019). Rational Design of Graphene-Supported Single-Atom Catalysts for Hydrogen Evolution Reaction. Advanced Energy Materials, 9, 1803689.
[58] Wang, Q., Zhao, Z. L., Dong, S., He, D., Lawrence, M. J., Han, S., Cai, C., Xiang, S., Rodriguez, P., Xiang, B., Wang, Z., Liang, Y. & Gu, M. (2018). Design of active nickel single-atom decorated MoS_2 as a pH-universal catalyst for hydrogen evolution reaction. Nano Energy, 53, 458–467.
[59] Cao, E., Chen, Z., Wu, H., Yu, P., Wang, Y., Xiao, F., Chen, S., Du, S., Xie, Y., Wu, Y. & Ren, Z. (2020). Boron-Induced Electronic-Structure Reformation of CoP Nanoparticles Drives Enhanced pH-Universal Hydrogen Evolution. Angewandte Chemie International Edition, 59, 4154–4160.
[60] Chen, L., Zhang, Y., Wang, H., Wang, Y., Li, D. & Duan, C. (2018). Cobalt-layered double hydroxides derived CoP/Co_2P hybrids for electrocatalytic overall water splitting. Nanoscale, 10, 21019–21024.
[61] Liu, H., Ma, X., Hu, H., Pan, Y., Zhao, W., Liu, J., Zhao, X., Wang, J., Yang, Z., Zhao, Q., Ning, H. & Wu, M. (2019). Robust NiCoP/CoP heterostructures for highly efficient hydrogen evolution electrocatalysis in alkaline solution. ACS Applied Materials & Interfaces, 11, 15528–15536.
[62] Huang, X., Xu, X., Luan, X. & Cheng, D. (2020). CoP nanowires coupled with CoMoP nanosheets as a highly efficient cooperative catalyst for hydrogen evolution reaction. Nano Energy, 68, 104332.
[63] Zhou, W., Jia, J., Lu, J., Yang, L., Hou, D., Li, G. & Chen, S. (2016). Recent developments of carbon-based electrocatalysts for hydrogen evolution reaction. Nano Energy, 28, 29–43.
[64] Duan, J., Chen, S., Jaroniec, M. & Qiao, S. Z. (2015). Porous C_3N_4 nanolayers@N-graphene films as catalyst electrodes for highly efficient hydrogen evolution. ACS Nano, 9, 931–940.
[65] Ito, Y., Cong, W., Fujita, T., Tang, Z. & Chen, M. (2015). High catalytic activity of nitrogen and sulfur co-doped nanoporous graphene in the hydrogen evolution reaction. Angewandte Chemie International Edition, 54, 2131–2136.
[66] Zheng, Y., Jiao, Y., Li, L. H., Xing, T., Chen, Y., Jaroniec, M. & Qiao, S. Z. (2014). Toward design of synergistically active carbon-based catalysts for electrocatalytic hydrogen evolution. ACS Nano, 8, 5290–5296.
[67] Wei, L., Karahan, H. E., Goh, K., Jiang, W., Yu, D., Birer, Ö., Jiang, R. & Chen, Y. (2015). A high-performance metal-free hydrogen-evolution reaction electrocatalyst from bacterium derived carbon. Journal of Materials Chemistry A, 3, 7210–7214.

[68] Zhao, Y., Zhao, F., Wang, X., Xu, C., Zhang, Z., Shi, G. & Qu, L. (2014). Graphitic carbon nitride nanoribbons: graphene-assisted formation and synergic function for highly efficient hydrogen evolution. Angewandte Chemie International Edition, 53, 13934–13939.
[69] Patra, B. C., Khilari, S., Manna, R. N., Mondal, S., Pradhan, D., Pradhan, A. & Bhaumik, A. (2017). A metal-free covalent organic polymer for electrocatalytic hydrogen evolution. ACS Catalysis, 7, 6120–6127.
[70] Niaz, S., Manzoor, T. & Pandith, A. H. (2015). Hydrogen storage: materials, methods, and perspectives. Renewable and Sustainable Energy Reviews, 50, 457–469.
[71] Ali, N. A. & Ismail, M. (2021). Modification of NaAlH4 properties using catalysts for solid-state hydrogen storage: a review. International Journal of Hydrogen Energy, 46, 766–782.
[72] Li, Z., Gao, M., Gu, J., Xian, K., Yao, Z., Shang, C., Liu, Y., Guo, Z. & Pan, H. (2020). In situ introduction of Li_3BO_3 and NbH leads to superior cyclic stability and kinetics of a LiBH4-based hydrogen storage system. ACS Applied Materials & Interfaces, 12, 893–903.
[73] Salehabadi, A., Salavati-Niasari, M. & Ghiyasiyan-Arani, M. (2018). Self-assembly of hydrogen storage materials based on multi-walled carbon nanotubes (MWCNTs) and Dy3Fe5O12 (DFO) nanoparticles. Journal of Alloys and Compounds, 745, 789–797.
[74] Suresh, K., Aulakh, D., Purewal, J., Siegel, D. J., Veenstra, M. & Matzger, A. J. (2021). Optimizing hydrogen storage in MOFs through engineering of crystal morphology and control of crystal size. Journal of the American Chemical Society, 143, 10727–10734.
[75] Tong, M., Zhu, W., Li, J., Long, Z., Zhao, S., Chen, G. & Lan, Y. (2020). An easy way to identify high performing covalent organic frameworks for hydrogen storage. ChemComm, 56, 6376–6379.